Retaining Short-term Variability Reduces Mean State Biases in Wind Stress Overriding Simulations

Matthew T. Luongo[1], Noel G. Brizuela[1,2], Ian Eisenman[1], & Shang-Ping Xie[1]

[1]Scripps Institution of Oceanography, UC San Diego, La Jolla, CA

[2]Lamont-Doherty Earth Observatory, Columbia University, New York, NY

Key Points:

- Most previous wind stress overriding simulations have disabled momentum feedbacks in global climate models by overriding with a climatology
- We introduce a protocol to override with interannually varying wind stress, which leads to smaller biases than climatological overriding
- We attribute this difference to a lack of synoptic variability in climatological overriding which shoals the mixed layer

Corresponding author: M.T. Luongo, `mluongo@ucsd.edu`

Abstract

Positive feedbacks in climate processes can make it difficult to identify the primary drivers of climate phenomena. Some recent global climate model (GCM) studies address this issue by controlling the wind stress felt by the surface ocean such that the atmosphere and ocean become mechanically decoupled. Most mechanical decoupling studies have chosen to override wind stress with an annual climatology. In this study we introduce an alternative method of interannually varying overriding which maintains higher frequency momentum forcing of the surface ocean. Using a GCM (NCAR CESM1), we then assess the size of the biases associated with these two methods of overriding by comparing with a freely evolving control integration. We find that overriding with a climatology creates sea surface temperature (SST) biases throughout the global oceans on the order of $\pm 1°C$. This is substantially larger than the biases introduced by interannually varying overriding, especially in the tropical Pacific. We attribute the climatological overriding SST biases to a lack of synoptic and subseasonal variability, which causes the mixed layer to be too shallow throughout the global surface ocean. This shoaling of the mixed layer reduces the effective heat capacity of the surface ocean such that SST biases excite atmospheric feedbacks. These results have implications for the reinterpretation of past climatological wind stress overriding studies: past climate signals attributed to momentum coupling may in fact be spurious responses to SST biases.

Plain Language Summary

Because the ocean influences the atmosphere and vice versa, chicken-or-egg type problems abound throughout the climate system. Some studies have addressed this by controlling the wind stress field felt by the ocean in climate models in order to mechanically decouple the ocean from the atmosphere and thus determine the surface ocean response to a change in momentum forcing. Most previous studies that override wind stress have fed the ocean a mean annual cycle; however, this method removes the effect of shorter-term events like storms. We compare how well overriding experiments, forced either with the mean annual cycle of wind stress or with year-to-year varying wind stress, agree with a freely evolving control simulation. We find substantially larger sea surface temperature (SST) biases in the simulation forced with the mean annual cycle of wind stress. We attribute these biases to the lack of short-term weather events which mix the surface ocean.

1 Introduction

Comprehensive global climate model (GCM) simulations of the coupled atmosphere-ocean system have been used to study the response of the climate to external forcings and to understand intrinsic modes of climate variability. However, interpreting results from comprehensive coupled GCMs is complex and can often give rise to chicken-or-egg problems, especially regarding whether the atmosphere is driving the ocean or vice versa. Often the answer is that both are driving each other. Employing a hierarchy of models, from the simplest two-layer quasi-geostrophic models to the most complex GCMs, and peeling off subsequent levels of complexity until ones arrives at the simplest configuration which explains the process of interest, is seen as the gold standard for bridging the gap between simulation and understanding (Held, 2005).

Many studies throughout the past two decades have highlighted the gap in the hierarchy of models between a comprehensive GCM where the atmosphere and ocean are dynamically coupled (AOGCM) and an atmospheric GCM that is thermodynamically coupled to a motionless mixed layer slab ocean model (e.g., Green & Marshall, 2017; Kang et al., 2020). The difference between these two modeling configurations might naïvely be considered the impact of atmospheric momentum forcing on the ocean. However, because the ocean dynamically responds to fluxes of both buoyancy and momentum, an intermediate step exists where the ocean is able to respond to anomalous fluxes of either buoyancy or momentum only and then feed back on the atmosphere. Recently, modeling studies have explored this niche through the use of partially decoupled GCM simulations where a certain flux into the ocean is specified rather than allowed to freely evolve.

The specific process of overriding wind stress such that the ocean cannot react to the freely evolving wind field, and thus the ocean is "mechanically decoupled" (Larson & Kirtman, 2015), is a common GCM partial decoupling approach. Despite the specified surface momentum flux, the ocean is still able to dynamically respond to anomalous buoyancy fluxes; as a result, wind stress overriding simulations sit squarely between fully coupled and slab ocean GCM studies and have played a central role in investigating how buoyancy and momentum forcing affect the ocean and climate system. This specific process of partially decoupling the ocean from the atmosphere via momentum forcing is variously referred to in the literature as "mechanical decoupling" or "wind stress overriding," and we use these terms interchangeably.

Mechanically decoupled simulations were initially used primarily to study the impact of El Niño-Southern Oscillation (ENSO) on the climate system because of the crucial role of mechanical coupling between wind stress and thermocline depth in the Bjerknes feedback (Bjerknes, 1969; Wyrtki, 1975). In a series of studies, Larson and Kirtman (2015, 2017, 2019) effectively suppressed ENSO variability by globally overriding surface ocean wind stress with a daily climatology (i.e., a day-of-year average across multiple years) to create a set of initial conditions without ENSO influences in order to study how coupled instabilities may lead to subsequent ENSO growth.

More recently, however, global climatological wind stress overriding has been used to study non-ENSO phenomena. These studies explore topics such as Pacific sea surface temperature (SST) variance (Larson, Vimont, et al., 2018), buoyancy-forced characteristics of the Atlantic Meridional Overturning Circulation (AMOC, Larson et al., 2020), cross-equatorial energy transport (F. Liu et al., 2021), extratropical atmospheric variability (Larson, Pegion, & Kirtman, 2018; Larson et al., 2022), and global warming (McMonigal et al., 2023). Other studies have explored similar topics including the Pacific Meridional Mode (PMM) and Indian Ocean meridional heat transport by overriding the wind stress with a climatology in the Equatorial Pacific only and allowing the wind stress to freely evolve elsewhere (Zhang et al., 2021; McMonigal & Larson, 2022).

While the vast majority of wind stress overriding simulations have used climatological overriding of some form, as described above, other schemes have also been occasionally used, such as overriding with wind stress from a repeating ENSO cycle (Larson & Kirtman, 2019) or adding specified anomalies to a climatology (Chakravorty et al., 2020, 2021). Other studies have supplied daily, interannually varying wind stress to the ocean from a separate integration where daily wind stress is output (Lu & Zhao, 2012; W. Liu et al., 2015, 2018; Luongo et al., 2022a, 2023; Fu & Fedorov, 2023). As opposed to overriding the total wind stress field in one model as discussed above, the flux anomaly forced model intercomparison project (FAFMIP: Gregory et al., 2016) specifies momentum anomalies to different model control states.

Overriding wind stress to decouple the ocean from the atmosphere invariably creates a climate bias relative to a control integration. We refer to this signature as the "decoupling bias." The question then arises as to how these wind stress overriding schemes differ in the size and pattern of their decoupling biases. In this study, we explore the ex-

tent to which the adopted decoupling scheme alone impacts the climate system. We focus primarily on climatological overriding, since this is the main decoupling protocol used in previous studies. We primarily present results from two GCM simulations meant to systematically explore the bias associated with each decoupling protocol compared with a freely evolving, fully coupled control case.

This paper is laid out as follows. Section 2 explains wind stress overriding methods, discusses the smoothing effects of climatological averaging on wind stress variability, and describes the GCM simulations used in this study. Section 3 describes the SST biases associated with the two overriding approaches and proposes possible drivers of the differences. We discuss implications for the results of past wind stress overriding studies in Section 4 and conclude in Section 5.

2 Wind Stress Overriding Simulations

We use the Community Earth System Model, Version 1.2 (CESM1: Hurrell et al., 2013) from the National Center for Atmospheric Research in its standard fully coupled configuration, which includes active atmosphere (CAM5: Neale et al., 2010), ocean (POP2: Smith et al., 2010), land surface (CLM4: Lawrence et al., 2012), and sea ice (CICE4: Holland et al., 2012) components that are interactively coupled by the model's coupler (Craig, 2014). Many previous wind stress overriding studies have also used versions of CESM (Larson & Kirtman, 2015; Larson et al., 2017; Larson, Vimont, et al., 2018; Larson et al., 2020; Chakravorty et al., 2020, 2021; F. Liu et al., 2021; McMonigal & Larson, 2022; Luongo et al., 2022a, 2023; McMonigal et al., 2023; Fu & Fedorov, 2023). In this study, we adopt the configuration used in Luongo et al. (2022a, 2023): the model is forced with standard pre-industrial forcing, and the atmosphere and land are run on a nominal 2° grid while the ocean and sea ice are run on a nominal 1° grid. Note that the model calendar has no leap years. We run one 51-year simulation, "Ctrl," in a fully coupled configuration and output daily wind stress for the subsequent overriding experiments, as explained below. We consider Ctrl as the reference "truth" throughout this study.

The basic concept of wind stress overriding and how it differs from a fully coupled model evolution is laid out schematically in Figure 1. At each coupling step in a fully coupled run, the ocean and atmosphere component models pass their state to the GCM coupler, which then computes buoyancy and momentum fluxes and passes them back to

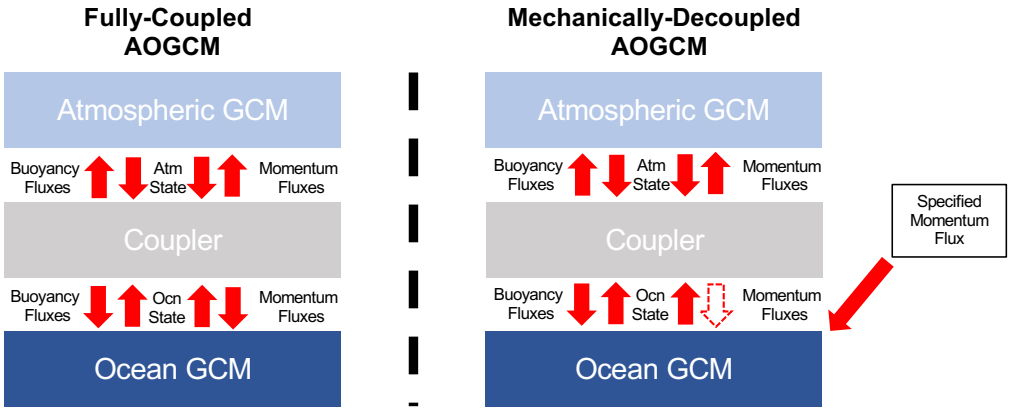

Figure 1. Schematic illustrating the difference between a fully coupled Atmosphere-Ocean-GCM (AOGCM) and a mechanically-decoupled AOGCM. In wind stress overriding experiments, the handoff between the coupler and the ocean is interrupted and the ocean is instead fed a specified momentum flux. All other flux coupling is retained.

the component models. Ocean coupling occurs daily in CESM. This hand-off between the coupler and the ocean is partially interrupted in wind stress overriding simulations such that the ocean is instead forced with a specified momentum flux field. While in principle one could alternatively approximately override wind stress by intercepting the hand-off from the atmosphere to the coupler before momentum fluxes are computed (W. Liu et al., 2018), most studies directly override in the ocean component to avoid any unwanted downstream effects. It should be noted that wind stress overriding only affects momentum fluxes into the ocean; turbulent heat fluxes, which use wind speed in bulk formulation, are retained as thermal fluxes into the surface ocean.

2.1 Climatological Overriding

Climatological overriding is the method most often employed to override wind stress in mechanical decoupling experiments. The basic assumption of climatological overriding is one of approximate linearity and can be stated as

$$\langle F(\vec{\tau})\rangle \approx F(\langle \vec{\tau}\rangle) \ . \tag{1}$$

Here angle brackets denote a climatological time averaging process to create a mean annual cycle from a multi-year record. Equation 1 indicates that the mean state of the climate, F, which is a function of wind stress, $\vec{\tau}$, is approximately equal to the state of cli-

Simulation Name	$\vec{\tau}$ Overriding Protocol
Ctrl	N/A: Freely evolving control case
ClimTau	Override wind stress with 50-year climatology.
FullTau	Override wind stress with interannually varying field.
ENSONeutralTau	Override wind stress with repeating neutral ENSO year.
ENSONegativeTau	Override wind stress with repeating negative ENSO year.
ENSOPositiveTau	Override wind stress with repeating positive ENSO year.

Table 1. The simulation name and description of the six simulations considered in this study. We primarily focus on the difference in the 50-year average climate response between each overriding method (Rows 2-6) and the fully coupled control case (Row 1). The specific years used in ENSONeutralTau, ENSONegativeTau, and ENSOPositiveTau are chosen based on the Nino 3.4 regional SST anomaly in Ctrl and are shown in Figure S3.

mate as a function of mean wind stress. We take the day-of-year average of daily wind stress data from years 1-50 of the Ctrl run to create a daily climatology of global wind stress. The "ClimTau" simulation is forced with this daily climatology for 50 years.

2.2 Interannually Varying Overriding

Taking a daily climatology averages out high frequency variability. The climatology retains the mean seasonal cycle, but synoptic and subseasonal variability are largely averaged out. This higher frequency wind stress forcing, which includes phenomena such as storms, may have important impacts on the mean ocean state due to processes such as upper ocean mixing (e.g., Brizuela et al., 2023). The degree to which Equation 1 fails to apply represents the degree of nonlinear rectification in the climate system (e.g., Huybers & Wunsch, 2003; Eisenman, 2012), i.e., the extent to which higher-frequency wind stress variability projects onto the longer-term ocean state.

Luongo et al. (2022a, 2023) used wind stress overriding to study the quasi-equilibrium upper ocean response to extratropical top-of-atmosphere aerosol-like radiative forcing. The authors mechanically decoupled the ocean from the atmosphere by overriding with a time evolving multi-year daily wind stress field, thereby maintaining full wind stress

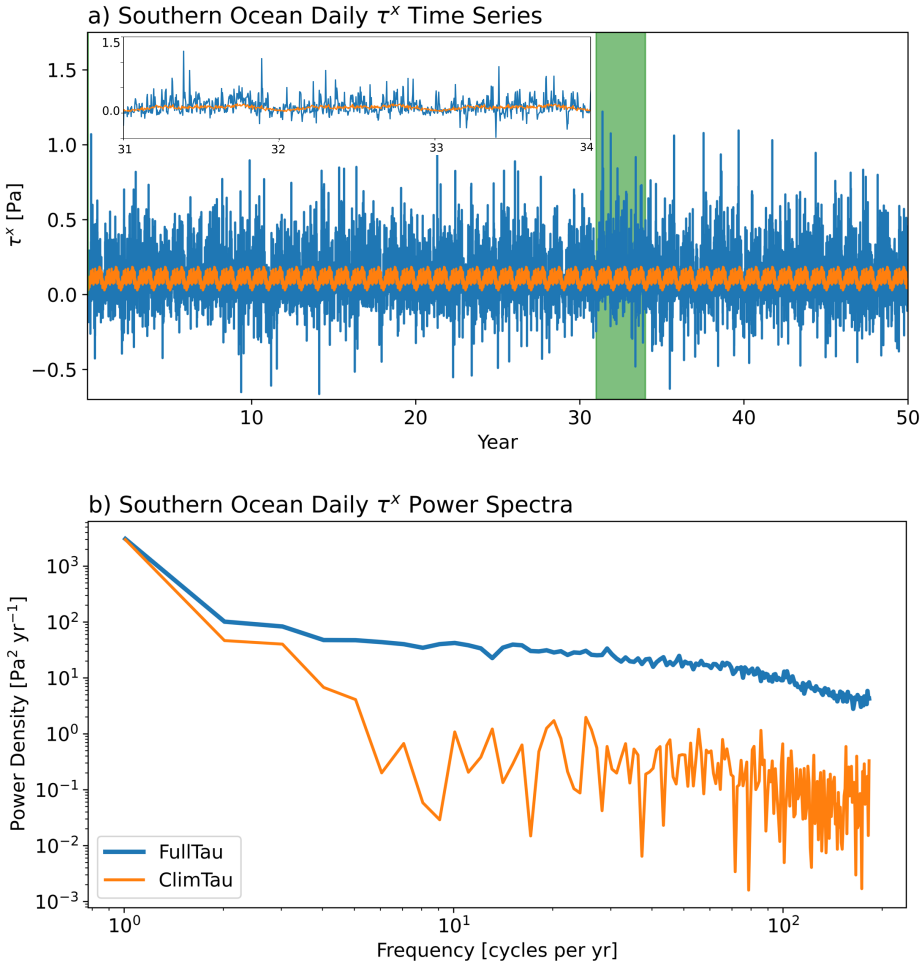

Figure 2. a) Time series of daily zonal wind stress, τ^x, from a specific location in the Southern Ocean (60°S, 25°W: yellow star in Figure 3b) for FullTau (blue) and ClimTau (orange). Years 31-34 of the simulation are highlighted in the inset. b) Power spectrum of daily zonal wind stress for FullTau and ClimTau. Both spectra are computed using Bartlett's Method by taking the average of one-year periodograms for each of the fifty years.

variability. Here we replicate this overriding scheme in the "FullTau" simulation. Note that wind stress in year n of the FullTau simulation is taken from year $n + 1$ of Ctrl, and that the 50-year FullTau simulation, which has the wind stress field specified from years 2-51 of Ctrl, is equivalent to the "Tau1S1" simulation in Luongo et al. (2022a). The one-year offset is imposed in order to circumvent the issue that if year n of FullTau was given wind stress from year n of Ctrl, then the two simulated climates would be precisely equal due to CESM's bit-for-bit reproducibility and the fact that our wind stress overriding technique is exact. Disrupting the temporal covariance between the atmosphere and ocean causes FullTau to be mechanically decoupled. All simulations analyzed in this study are described in Table 1.

This interannually varying overriding method requires management of daily wind stress fields for the full duration of the target overriding simulation, whereas climatological overriding requires management of just one year of wind stress fields. However, in our case of standard resolution CESM on the Cheyenne supercomputing system, the storage cost for 51 years of daily coupler files from Ctrl, which includes all surface flux fields passed from the coupler to the ocean, is 650 GB. This is less than the storage cost for the monthly atmospheric and ocean data fields generated by the 51 year Ctrl (720 GB).

Figure 2a plots the zonal component of daily wind stress, τ^x, at a specific location in the Southern Ocean (60°S, 25°W: yellow star in Figure 3b) for FullTau (blue) and ClimTau (orange). The daily values of τ^x in FullTau vary considerably on daily to interannual timescales, while the variability of τ^x in ClimTau is markedly suppressed with strong wind stress events associated with weather essentially removed. Frequency spectra (Figure 2b) further describe the difference between FullTau and ClimTau. We use Bartlett's Method to compute the spectra of τ^x in both FullTau and ClimTau: we compute the periodogram for each year in the 50-year span (after removing the mean and linear trend from the full time series), and then we take the average of the 50 spectra. The power spectra of these two Southern Ocean τ^x time series clearly show that ClimTau exhibits substantially less energy across timescales than FullTau. Unsurprisingly, there is a stark difference in wind stress variance between the two simulations throughout the Southern Ocean and in vast areas of the North Atlantic and North Pacific as well (Figure 3a & b). As discussed further in Section 3.2, the lack of temporal variability in ClimTau indicates that the sur-

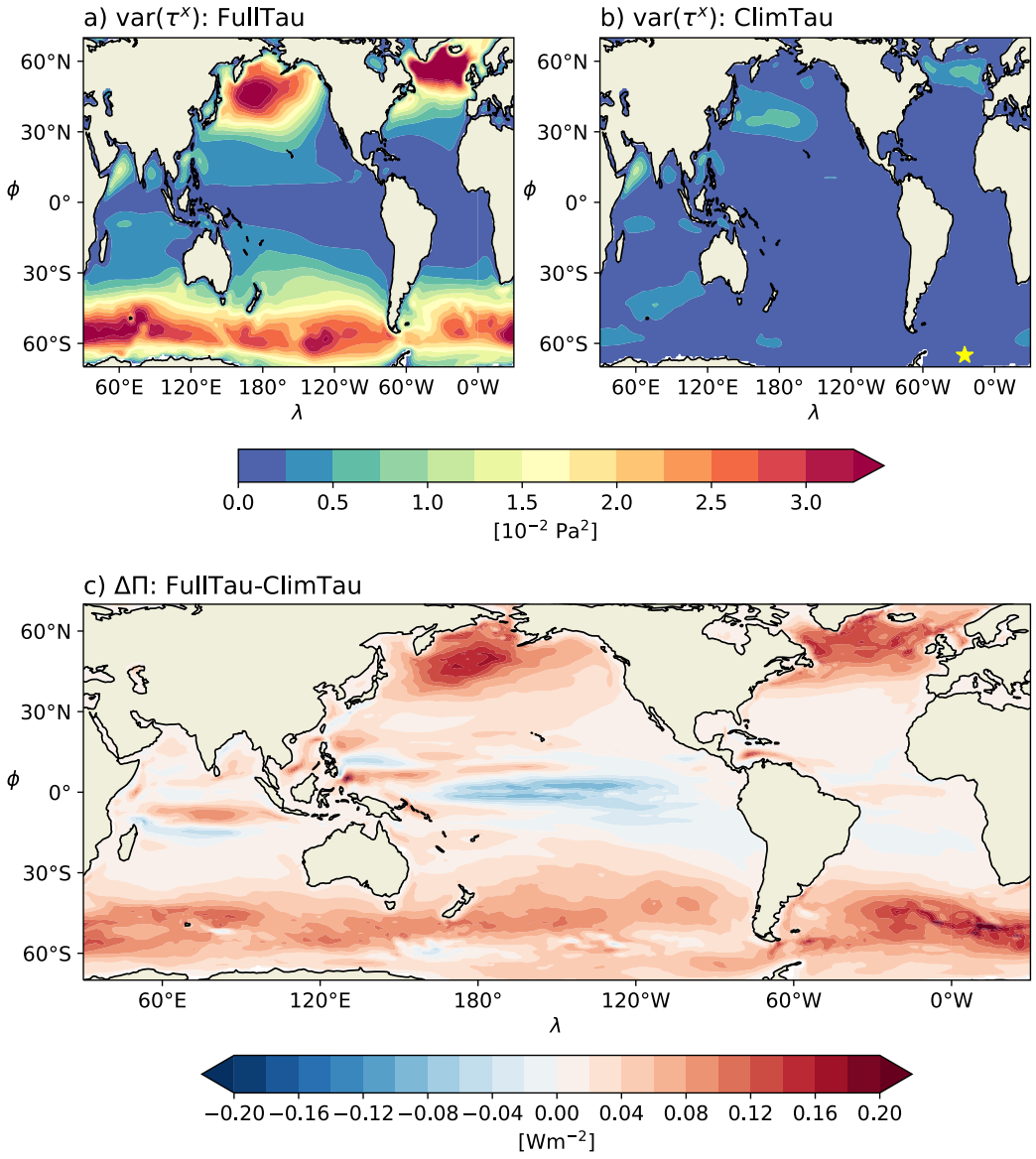

Figure 3. Top row: Variance in daily zonal wind stress, τ^x, in FullTau (a) and ClimTau (b). The yellow star in panel b indicates the location of the data presented in Figure 2. Bottom row: Difference in wind work, Π, between the FullTau and ClimTau simulations.

face ocean will receive less kinetic energy flux in the case of climatological wind stress overriding than it otherwise would in Ctrl.

3 Results

3.1 SST Response

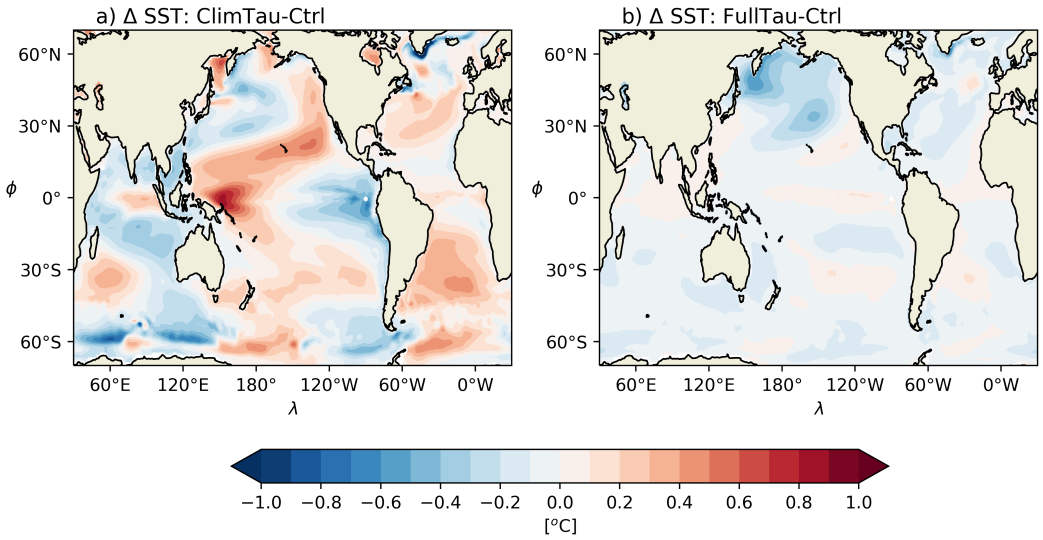

Figure 4. SST bias between (a) ClimTau and Ctrl and (b) FullTau and Ctrl averaged over the 50-year simulations.

The globally averaged SST time series of ClimTau and FullTau do not show appreciable drift away from Ctrl (Figure S1). However, climatological decoupling creates local SST residuals throughout the global oceans on the order of ±1°C (Figure 4a). Note that this pattern holds for seasonal averages as well (Figure S2). In contrast, the local SST residuals created by interannually varying wind stress overriding (Figure 4b) are considerably smaller, except for a patch of negative SST anomalies in the North Pacific on the poleward side of the Aleutian low. This cool patch, which is significantly different from Ctrl at the 95% level using a Student's t-test, occurs in three ensemble members (not shown), suggesting that it is a robust physical bias inherent to the FullTau setup. Regardless of what caused this cool patch— plausibly a change in the Kuroshio or the disruption of the positive covariance between turbulent and Ekman fluxes in the North Pacific westerly regime— the cooling can be communicated globally through atmospheric processes. This may explain why outside of this cool patch, the FullTau biases are neg-

ative nearly everywhere. The ClimTau SST biases, on the other hand, are significantly different from Ctrl at the 95% level across the entirety of the surface ocean (not shown) and consist of both positive and negative values. ClimTau SST biases in the North Pacific, the equatorial Indo-Pacific, the North Atlantic, and the Southern Ocean are particularly noteworthy (Figure 4a). Note that although the deep ocean would continue to adjust for far longer than these 50-year simulations, these surface bias patterns are relatively steady and experience a drift of only $< 0.005°C/yr$ in the last 20 years of the 50-year simulations (not shown).

The pattern and amplitude of the SST bias in the North Pacific is reminiscent of the positive phase of the Pacific Decadal Oscillation (PDO: Mantua & Hare, 2002), with cool SST anomalies in the Kuroshio Extension region and warm SST anomalies along the California coast. Larson et al. (2022) find a similar bias pattern between their fully coupled and climatological overriding simulations (their Figure 5). They use a third simulation where climatological wind stress overriding is only applied in the Equatorial Pacific to show that this positive PDO-like SST pattern partially results from air-sea heat flux anomalies in the absence of ENSO. However, this difference only accounts for a portion of the bias observed in Larson et al. (2022), with the remaining SST bias attributed to non-ENSO momentum dynamics and air-sea heat fluxes. Because the act of wind stress overriding disables a coupled ENSO regardless of the methodology used, and because we only find this PDO-like SST bias pattern in ClimTau, the full bias discussed in Larson et al. (2022) may be partially explained as an artifact of the decoupling technique used.

The warm SST anomalies in ClimTau extend from the subtropics southwestward along the PMM path into the tropics, where the resemblance to the positive PDO is lost. In fact, the clear zonal SST dipole in the Equatorial Pacific is somewhat reminiscent of a negative PDO; the Western Equatorial Pacific (WEP) experiences relatively strong warming and the Eastern Equatorial Pacific (EEP) experiences relatively strong cooling. Ogata et al. (2013) suggest that ENSO variability rectifies the interdecadal mean state of the tropical Pacific, and these biases may result from the lack of interannual variability in ClimTau because the SST bias pattern of warmer WEP and cooler EEP in ClimTau corresponds to suppressed ENSO amplitude. Consistent with this, FullTau has ENSO-like interannual thermocline variability, although it does not have interactive ENSO, and it does not have these equatorial SST dipole biases. A similar zonal SST dipole exists in the Indian Ocean where the Eastern Indian Ocean warms and the Western Indian Ocean

cools. As a quantitative point of comparison, the EEP SST difference in ClimTau is of a similar magnitude as the EEP SST response found by Luongo et al. (2023), where the climate was forced by a strong insolation reduction in the region $45° - 65°$N. Despite a disabled Bjerknes feedback and even without canonical ENSO variability, these tropical SST biases can still excite anomalous ocean circulation, turbulent heat fluxes at the ocean surface, and large-scale atmospheric circulation responses which can anchor these anomalies in place. In turn, these equatorial anomalies may then affect the subtropics via evaporative heat fluxes retained in mechanically decoupled simulations (e.g., Chiang & Vimont, 2004; Luongo et al., 2023), subsurface ocean ventilation (e.g., Burls et al., 2017; Heede et al., 2020), or changes in deep convection (e.g., Hoskins & Karoly, 1981).

The schematic of wind stress overriding in Figure 1 does not address how the wind stress is treated in regions that have sea ice, and neither wind stress overriding scheme perfectly deals with a potential climate jump at the sea ice edge. Comparison of ClimTau and FullTau SST residuals in the North Atlantic and Southern Ocean suggest that ClimTau SST biases in these regions, which exhibit a pronounced seasonality (Figure S2), are likely more complex than simply a result of sea ice effects. These anomalous SST patterns and resulting anomalous buoyancy fluxes cause ocean circulation adjustment and restratification, including in areas of deep convection such as the Labrador and Weddell Seas.

Although the present analysis only focuses on wind stress overriding in coupled GCMs, it is worth briefly considering previous studies that used similar approaches in ocean-only GCMs. For instance, while many studies force ocean GCMs with a wind stress climatology (e.g., Peng et al., 2022), ocean-only FAFMIP (OFAFMIP: Todd et al., 2020) found that overriding with a climatology created biases relative to coupled GCM control simulations and so instead specified interannually varying daily surface momentum fluxes. Similarly, a number of previous ocean-only GCM studies have looped the wind stress field from a specific year to investigate buoyancy impacts on ocean circulation (Luo et al., 2015; F. Liu et al., 2017). While this method maintains the effects of synoptic and subseasonal variability on the surface ocean, any peculiarities of the year chosen can strongly imprint on the mean simulated climate state. To explore the implications of using this as a coupled GCM overriding method, we take wind stress fields from a neutral, negative, and positive ENSO year in Ctrl, as defined by the Nino 3.4 SST index (Figure S3a). We run three additional 50-year simulations, "ENSONeutralTau," "ENSONegativeTau," and "ENSOPositiveTau," each forced by repeating the wind stress from a different sin-

gle year. SST biases using this overriding method are much larger than in either ClimTau or FullTau (Figure S3b-g), and the specific patterns vary depending on which year is chosen within an ENSO cycle. These results suggest that overriding with a single repeating year leads to strikingly large biases and does not accurately recreate the mean state of the surface ocean.

3.2 Possible Mechanisms for Bias in ClimTau

The rate of kinetic energy input from winds into the surface ocean velocity field, often called "wind work," is given by the inner product of the wind stress and the surface ocean velocity,

$$\Pi = \vec{\tau} \cdot \vec{u} \, . \tag{2}$$

Because the surface velocity field can be decomposed into geostrophic and ageostrophic components, $\vec{u} = \vec{u}_g + \vec{u}_{ag}$, Π can also be decomposed similarly, $\Pi = \Pi_g + \Pi_{ag}$. Π_g is a main driver of large-scale ocean circulation and a major source of mechanical energy for the deep ocean (e.g., Oort et al., 1994; Munk & Wunsch, 1998; Wunsch & Ferrari, 2004; Ferrari & Wunsch, 2009). Wunsch (1998) used reanalysis winds and satellite altimeter data to compute 10-day averages of $\vec{\tau}$ and $\vec{u}_g$ and solve for a global estimate of Π_g of about 1 TW. Subsequent studies have generally confirmed $\Pi_g \approx 1$ TW and that most of this work is done in the Southern Ocean by the zonal component of the time-averaged wind stress on the time-averaged geostrophic surface velocity (Huang et al., 2006; Hughes & Wilson, 2008; Scott & Xu, 2009; Zhai et al., 2012).

However, considering that synoptic storms make up some of the most prominent peaks in the time series of Π (Alford, 2001), Π_{ag} associated with synoptic events likely substantially contributes to global estimates of Π. Indeed, in GCM diagnoses, von Storch et al. (2007) and Gregory and Tailleux (2011) used actual simulated $\vec{\tau}$ and $\vec{u}$ and evaluated total $\Pi \approx 3 - 4$ TW, further establishing that only considering Π_g gives a substantial underestimate of total mechanical energy input to the surface ocean. Wang and Huang (2004) use a classical Ekman spiral solution to solve for Π_{ag} and, in addition to power estimates of near-inertial motions (e.g., Alford, 2001), suggest $\Pi_{ag} \approx 2{-}3$ TW. Elipot and Gille (2009) show that the primary contributor to Π_{ag} is the covariance of wind stress and surface velocities and, according to Wang and Huang (2004), Π_{ag} is spent supporting turbulence and mixing to maintain upper ocean velocity and stratification

fields. Because FullTau has a much larger wind stress variance than ClimTau (c.f. Figure 3a & b), FullTau should also have a larger Π_{ag} than ClimTau. While a full decomposition into Π_g and Π_{ag} is beyond the scope of this work, Figure 3c presents the difference in total Π between FullTau and ClimTau and shows nearly uniform positive values poleward of the deep tropics. This difference between the two simulations likely results from the difference in Π_{ag} associated with the preservation of high frequency wind stress variability (Figure 2b). In particular, FullTau experiences substantially more wind work than ClimTau in regions with high wind stress variance such as the Southern Ocean and the Northern Hemisphere storm tracks.

Figure 3c clearly shows that the lack of synoptic variability in ClimTau leads to a less energetic surface ocean across much of the globe and therefore less energy available to sustain realistic levels of near-surface mixing. Indeed, the mixed layer depth (MLD) in ClimTau is substantially shallower than Ctrl throughout much of the global ocean (Figure 5a). In particular, the mixed layer is biased too shallow in nearly all extratropical regions outside of 30°S to 30°N. These MLD patterns qualitatively match the global pattern of the daily wind stress variance and the difference in Π between FullTau and ClimTau (Figure 3), indicating the critical role of synoptic variability in maintaining the MLD in these extratropical regions.

Suppressed wind stress variance associated with winter and spring synoptic storms seem to play a key role in the annual mean MLD response: the too shallow MLD signature in the Northern Hemisphere is strongest in boreal winter and spring, while the too shallow MLD signature in the Southern Hemisphere is strongest in austral winter and spring (Figure S4). The ClimTau MLD bias is smaller throughout much of the tropics, which is also the region with the lowest daily wind stress variance (Figure 3a & b). However, a shallow MLD signal does exist in the tropical Indo-Pacific around the maritime continent in the ClimTau experiment, which may be locally related to disabled ENSO variability or perhaps to the lack of synoptic tropical cyclone-like activity. On the other hand, with the exception of the far North Atlantic, there are minimal differences between MLD in FullTau and Ctrl throughout much of the ocean (Figure 5b). The too deep MLD bias in the North Atlantic may result from changes in the AMOC caused by the lack of covariance between the surface ocean and high frequency stochastic wind stress forcing or from geographic shifts in the locations of deep convection.

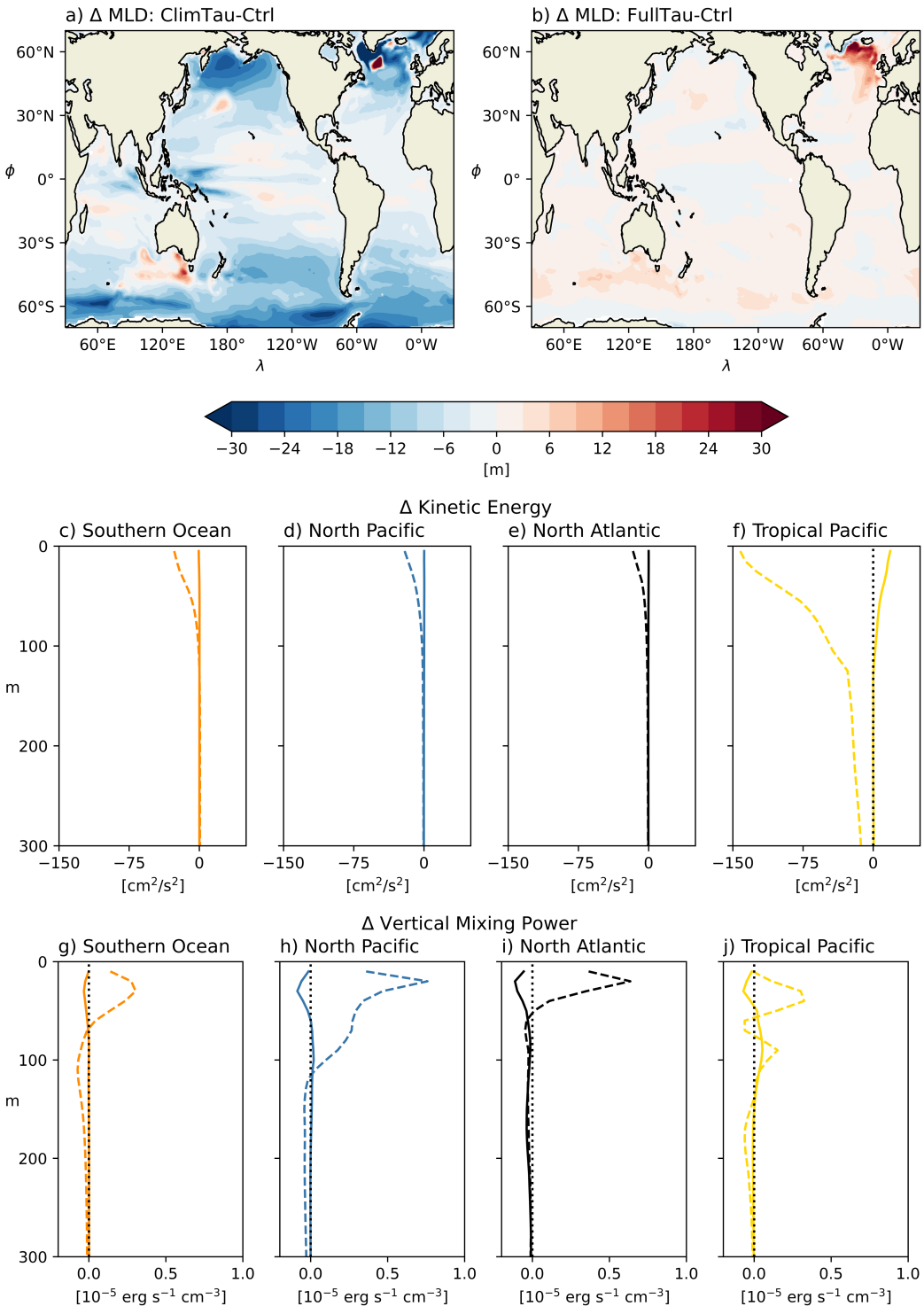

Figure 5. Top row: 50-year average mixed layer depth (MLD) bias between (a) ClimTau and Ctrl and (b) FullTau and Ctrl. Middle row: 50-year regional average depth profile of horizontal kinetic energy bias between ClimTau and Ctrl (dashed lines) and FullTau and Ctrl (solid lines). Bottom row: 50-year regional average depth profile of vertical mixing power bias between ClimTau and Ctrl (dashed lines) and FullTau and Ctrl (solid lines).

The lack of synoptic variability in ClimTau has a notable impact on area-averaged depth profiles of near-surface horizontal kinetic energy biases. Figures 5c-f show that climatological overriding causes a decrease in near-surface kinetic energy over the Southern Ocean (orange dashed line), North Pacific (blue dashed line), North Atlantic (black dashed line), and tropical Pacific (dashed yellow line). In the extratropics, the negative near-surface kinetic energy bias in ClimTau likely results from the decreased wind work seen in Figure 3c. On the other hand, the decrease in tropical Pacific kinetic energy is substantially larger than in the extratropical regions. Because ClimTau experiences smaller wind stress variance biases in the tropics, this difference is likely primarily a result of reduced ENSO variability rather than reduced synoptic variability. Meanwhile, the difference in near-surface kinetic energy profiles between FullTau and Ctrl (Figure 5c-f: solid lines, same colors) are near zero in non-tropical regions. In the tropical Pacific, however, the difference in the kinetic energy bias profile is positive and nearly the same magnitude as ClimTau's North Pacific bias. This may result from the disruption of the covariance between wind stress and surface currents in the equatorial region, where surface currents can damp changes in wind stress (Seo et al., 2023). This bias is likely also related to the decreased Π observed in the tropics in FullTau (Figure 3c). Though changes in kinetic energy profiles could in principle be caused by factors other than changes in wind stress (e.g., anomalous buoyancy fluxes), CESM diagnostically reports monthly total volume-integrated kinetic energy, and changes to total kinetic energy from wind stress are consistently an order of magnitude larger than other changes (not shown).

The decrease of wind work and near-surface kinetic energy in ClimTau is related to changes in vertical mixing power (the "TPOWER" variable in CESM). CESM uses the K-profile parameterization scheme (Large et al., 1994; Danabasoglu et al., 2006) to solve for vertical mixing power as the product of parameterized vertical diffusivity, density, and the vertical buoyancy gradient. Here, diffusivity depends on atmospheric forcing and near-surface ocean current shear such that changes in wind stress between FullTau and ClimTau change both the flow field and the diffusivity and thereby change the vertical mixing power. In turn, vertical mixing power is equal to the rate of work done against gravity to transport buoyancy within the mixed layer to reduce the vertical buoyancy gradient. Because heat absorbed by the ocean will stay close to the surface unless mechanical energy stirs it deeper, a change in vertical mixing power will affect heat transport between the surface mixed layer and the thermocline. Figures 5g-j show an increase

in vertical mixing power in ClimTau just below the surface in all regions and a decrease in vertical mixing power at greater depths. This response implies that most of the available mixing energy in ClimTau is spent mixing areas near the surface which are largely homogeneous in FullTau and Ctrl. Meanwhile, decreased vertical mixing in the thermocline suggests less of a connection between the mixed layer and colder thermocline waters below. Near-surface FullTau vertical mixing profile biases are slightly negative which may plausibly have to do with diffusivity changes as a result of the near-uniform cooling bias observed in FullTau (Figure 4b).

The bias toward too shallow MLD values in ClimTau has substantial implications for the surface ocean-atmosphere coupled system. By reducing the MLD, climatological wind stress overriding reduces the effective heat capacity of the surface ocean. The reduced effective heat capacity of the surface ocean is expected to reduce the coupling time scales between the atmosphere and ocean. Hence, the shallow MLD in ClimTau is expected to allow anomalous mixed layer heat to rapidly change SST locally, whereas the synoptic variability in Ctrl provides sufficient kinetic energy to mix anomalous heat into the thermocline. Anomalous SSTs in ClimTau may then trigger atmospheric responses which can amplify anomalies further. We note, for instance, the clear PMM patterns in both hemispheres of the subtropical Pacific (Figure 4a), where evaporative cooling dominates the surface heat budget, which persist throughout the year (Figure S2). SST anomalies in the extratropics, where synoptic variability is key to maintaining a realistic ocean state, can go on to affect the tropics, where synoptic variability may be less important, either through surface pathways mediated by cloud feedbacks and the Northern or Southern PMM (e.g., Dong et al., 2022; Luongo et al., 2023) or through subsurface ocean circulation adjustment of the subtropical cells (Burls et al., 2017; Heede et al., 2020). Once in the tropics, SST anomalies can trigger anomalous deep convection and affect the extratropics (Hoskins & Karoly, 1981). In addition, by not mixing as much heat into the thermocline, ClimTau likely differs from Ctrl in the amount of heat that could otherwise reemerge remotely through ocean dynamics (Jansen et al., 2010; Brizuela et al., 2023). Overall, we find that climatological wind stress overriding leads to a shallower MLD and a less energetic near-surface ocean such that anomalous heat fluxes into the mixed layer may be expected to affect SST more rapidly.

4 Discussion

In the preceding section, we showed that climatological wind stress overriding simulations develop spurious temperature responses due to insufficient wind-driven mechanical energy input into the near-surface ocean. Although some prior studies have shown the mean state climate biases generated by their choice of wind stress overriding technique, here we have systematically compared the magnitude and pattern of SST biases created by two methods of wind stress overriding. Through this comparison we highlighted important differences between the two methods, which may be useful to inform future overriding studies.

We emphasize two central points associated with these results. First, decoupling biases exist in all wind stress overriding studies regardless of the overriding technique used. This mean state bias is especially relevant whenever the mean state of a fully coupled simulation is compared with that of a mechanically decoupled simulation. A number of previous studies have based their conclusions on such comparisons. For example, F. Liu et al. (2021) heated the Southern Ocean in CESM1 and then compared the fully coupled response with the response from a simulation under the same forcing but with climatological wind stress overriding. The near-surface differences in temperature, which they ascribe to wind stress forcing, are smaller than the biases that we find to be introduced via climatological overriding (c.f. Figure 4a with their Figure 8). In a similar vein, McMonigal et al. (2023) simulate greenhouse warming in CESM2 with and without climatological wind stress overriding and conclude that wind-driven changes accelerate greenhouse warming. Although their overriding bias pattern, defined here as their unforced mechanically decoupled simulation minus their unforced control simulation, differs from what we find in CESM1 (c.f. Figure 4a with their Figure S1 with the sign reversed), in general their bias show a nearly-uniform warming of around 1^oC, which is the same order as what they attribute to the role of wind stress forcing in greenhouse warming (their Figure 4).

This bias can be explained using a simple example. Consider a situation where greenhouse forcing is applied in a fully coupled CESM1 simulation and that simulation is then compared with a simulation that has the same greenhouse forcing but overrides wind stress with the interannually varying wind stress from an unforced control simulation. If we compared these two simulations directly, the near uniform cooling seen in Figure 4b would

project onto what would be considered the forced response. This would add a near uniform warming of the globe to the actual effect of wind stress changes associated with global warming. In other words, part of the simulated signal would be a spurious decoupling bias. Similarly, if the same analysis is instead carried out using climatological wind stress overriding [as in F. Liu et al. (2021) and McMonigal et al. (2023)], the spurious tropical Pacific zonal dipole biases in Figure 4a would be added to the actual effect of wind stress changes. This could readily lead to inaccurate conclusions regarding the tropical response associated with global warming. When exploring an externally forced response, such as greenhouse or aerosol forcing, a direct way to address this issue of mean state bias is by comparing two mechanically decoupled simulations. To the extent that the system responds linearly, differencing a mechanically decoupled simulation from another mechanically decoupled simulation will remove mean state biases. This method of comparing a forced mechanically decoupled simulation with an unforced mechanically decoupled control was suggested by Lu and Zhao (2012) and adopted in some subsequent studies (W. Liu et al., 2015, 2018; Luongo et al., 2022a, 2023; Fu & Fedorov, 2023).

The second central point relates to the potential impact of wind stress overriding mean state biases on climate variability: decoupling biases in the mean state can have major global impacts if they affect large-scale modes of variability (e.g., Richter et al., 2018). For instance, ClimTau mean state biases are most strikingly different from FullTau in the tropical Pacific, where there is an approximately 2^oC spurious zonal temperature gradient. This ENSO-like zonal dipole has been observed to arise from decadal atmospheric forcing of slab ocean simulations (Clement et al., 2011; Okumura, 2013) and can then affect extratropical variability through atmospheric teleconnections. As such, in studies which have used wind stress overriding to investigate internal variability outside of the Equatorial Pacific (e.g., Larson, Vimont, et al., 2018; Zhang et al., 2021; Larson et al., 2022), tropical SST biases from overriding may alter extratropical variability in a way that is not equivalent to what could be ascribed to ENSO forcing alone. This suggests that the difference between climate variability in a fully coupled simulation and a climatological overriding simulation can not be interpreted as entirely attributable to the effect of ENSO on the climate system. Instead, differences may be a combination of both ENSO forcing and how these spurious effects of decoupling impact climate variability, and pinpointing exactly which of these responses dominates requires careful experimental design. Though this second consideration is relevant to all wind stress overrid-

ing simulations, it is reasonable to assume that reducing biases as much as possible helps with this issue.

Although we find that climatological wind stress overriding produces substantially larger biases than interannually varying wind stress overriding when compared with a control simulation, we note that there are situations where climatological wind stress overriding is preferable to interannually varying wind stress overriding. For instance, interannual wind stress variability in the prescribed wind stress field can still affect the thermocline to create an uncoupled ENSO-like response in the interannually varying overriding scheme. As result, interannually varying overriding would be an inappropriate tool to remove ENSO variability as initially accomplished by Larson and Kirtman (2015). Because the two methods are only interchangeable in so far as they both disable momentum feedbacks between the atmosphere and ocean, the ultimate choice of wind stress overriding technique depends on the scientific question at hand. In general, climatological overriding works well for scientific questions which depend on the mean wind stress seasonal cycle and where higher frequency variability obscures the signal [e.g., the role of instabilities in ENSO initiation (Larson & Kirtman, 2015, 2017, 2019)]. On the other hand, interannually varying overriding works well for scientific questions which require a realistic upper ocean state or smaller decoupling biases.

5 Conclusion

In this study we investigate the biases generated in wind stress overriding simulations where the atmosphere is mechanically decoupled from the ocean in a coupled GCM. We find that the biases relative to a fully coupled control simulation in a mechanically decoupled simulation with climatological wind stress overriding are substantially larger than the biases in a mechanically decoupled simulation which uses interannually varying overriding. The climatological wind stress overriding biases take the form of familiar patterns of surface ocean and atmosphere variability, such as meridional modes and atmospherically forced ENSO-like and Indian Ocean Dipole-like zonal dipoles. However, these bias patterns are absent in the simulations with interannually varying wind stress overriding, showing that these biases do not merely represent the influence of momentum coupling on the surface ocean. These biases are present in past climatological wind stress overriding studies and are especially relevant when comparing the forced response

of a fully coupled and mechanically decoupled simulation and if the mean state biases appreciably affect extratropical climate variability.

Although we focus on SST residuals in this study, similar differences occur in other climate variables as well (e.g., net surface heat flux, precipitation, and sea level pressure; not shown). We find that the substantial bias in climatological overriding occurs because climatological overriding removes synoptic and subseasonal variability. This lack of high frequency variability in the climatological wind stress overriding simulations leads to shoaling of the ocean mixed layer throughout the extratropical region, which otherwise experiences high day-to-day wind stress variance. We find that the near-surface ocean in climatological overriding simulations is characterized by reduced kinetic energy, too much vertical mixing at the surface, and not enough vertical mixing at depth.

While simulations forced with climatological wind stress were initially used as an effective means to remove the influence of ENSO on the climate, many subsequent studies have used climatological overriding to study extratropical variability and forced climate responses. As measured by the size of the bias compared with a fully coupled simulation, the results of the present study suggest that climatological overriding does not create as realistic of an ocean state as when an interannually varying wind stress field is used. We find that climatological overriding adds SST biases on the order of $\pm 1^{\circ}$C throughout the global ocean while interannually varying overriding leads to considerably smaller biases nearly everywhere. By directly comparing these two overriding methods, we emphasize the importance of matching the overriding technique with the scientific question at hand to minimize the impact of decoupling effects on the scientific phenomenon being investigated. These results provide context for potential reinterpretation of past climatological overriding studies and lay a foundation for future wind stress overriding studies and their bias tolerance.

6 Open Research

The interannually varying wind stress overriding protocol for CESM is available through the UCSD library digital collections (Luongo et al., 2022b). The climatological overriding protocol will be hosted by the UCSD library digital collections upon study publication. The data used to create Figures 2-5 have been uploaded for this initial sub-

mission as .mat files; they will be made freely available from the UCSD library digital collections upon publication.

Acknowledgments

This work was supported by NASA FINESST Fellowship 80NSSC22K1528 and NSF grant OCE-2048590. We thank UCAR and NSF for providing the graduate student allocation of core hours on Cheyenne that this research used and we thank the Extratropical-Tropical Interaction Model Intercomparison Project group for making their restart files available. Without implying their endorsement, we thank Clara Deser, Matthew H. Alford, Momme Hell, and Bruce Cornuelle for helpful discussions and suggestions. We also thank our editor, Dr. Stephen Griffies, and three anonymous reviewers for their thoughtful and constructive feedback which greatly improved this study.

References

Alford, M. H. (2001). Internal swell generation: The spatial distribution of energy flux from the wind to mixed layer near-inertial motions. *Journal of Physical Oceanography*, *31*(8), 2359–2368.

Bjerknes, J. (1969). Atmospheric teleconnections from the equatorial Pacific. *Monthly Weather Review*, *97*(3), 163–172.

Brizuela, N. G., Alford, M. H., Xie, S.-P., Sprintall, J., Voet, G., Warner, S. J., ... Moum, J. N. (2023). Prolonged thermocline warming by near-inertial internal waves in the wakes of tropical cyclones. *Proceedings of the National Academy of Sciences*, *120*(26), e2301664120.

Burls, N. J., Muir, L., Vincent, E. M., & Fedorov, A. (2017). Extra-tropical origin of equatorial Pacific cold bias in climate models with links to cloud albedo. *Climate Dynamics*, *49*(5), 2093–2113.

Chakravorty, S., Perez, R. C., Anderson, B. T., Giese, B. S., Larson, S. M., & Pivotti, V. (2020). Testing the trade wind charging mechanism and its influence on ENSO variability. *Journal of Climate*, *33*(17), 7391–7411.

Chakravorty, S., Perez, R. C., Anderson, B. T., Larson, S. M., Giese, B. S., & Pivotti, V. (2021). Ocean dynamics are key to extratropical forcing of El Niño. *Journal of Climate*, *34*(21), 8739–8753.

Chiang, J. C., & Vimont, D. J. (2004). Analogous Pacific and Atlantic meridional

modes of tropical atmosphere–ocean variability. *Journal of Climate*, *17*(21), 4143–4158.

Clement, A., DiNezio, P., & Deser, C. (2011). Rethinking the ocean's role in the Southern Oscillation. *Journal of Climate*, *24*(15), 4056–4072.

Craig, A. (2014). CPL7 user's guide. *Updated for CESM version*, *1*(6).

Danabasoglu, G., Large, W. G., Tribbia, J. J., Gent, P. R., Briegleb, B. P., & McWilliams, J. C. (2006). Diurnal coupling in the tropical oceans of CCSM3. *Journal of Climate*, *19*(11), 2347–2365.

Dong, Y., Armour, K. C., Battisti, D. S., & Blanchard-Wrigglesworth, E. (2022). Two-way teleconnections between the Southern Ocean and the tropical Pacific via a dynamic feedback. *Journal of Climate*, *35*(19), 6267–6282.

Eisenman, I. (2012). Factors controlling the bifurcation structure of sea ice retreat. *Journal of Geophysical Research: Atmospheres*, *117*(D1).

Elipot, S., & Gille, S. T. (2009). Estimates of wind energy input to the Ekman layer in the Southern Ocean from surface drifter data. *Journal of Geophysical Research: Oceans*, *114*(C6).

Ferrari, R., & Wunsch, C. (2009). Ocean circulation kinetic energy: Reservoirs, sources, and sinks. *Annual Review of Fluid Mechanics*, *41*(1), 253–282.

Fu, M., & Fedorov, A. (2023). The role of Bjerknes and shortwave feedbacks in the tropical Pacific SST response to global warming. *Geophysical Research Letters*, *50*(19), e2023GL105061.

Green, B., & Marshall, J. (2017). Coupling of trade winds with ocean circulation damps ITCZ shifts. *Journal of Climate*, *30*(12), 4395–4411.

Gregory, J. M., Bouttes, N., Griffies, S. M., Haak, H., Hurlin, W. J., Jungclaus, J., ... others (2016). The flux-anomaly-forced model intercomparison project (FAFMIP) contribution to CMIP6: Investigation of sea-level and ocean climate change in response to CO_2 forcing. *Geoscientific Model Development*, *9*(11), 3993–4017.

Gregory, J. M., & Tailleux, R. (2011). Kinetic energy analysis of the response of the Atlantic meridional overturning circulation to CO_2-forced climate change. *Climate Dynamics*, *37*, 893–914.

Heede, U. K., Fedorov, A. V., & Burls, N. J. (2020). Time scales and mechanisms for the tropical Pacific response to global warming: A tug of war between the

ocean thermostat and weaker Walker. *Journal of Climate*, *33*(14), 6101–6118.

Held, I. M. (2005). The gap between simulation and understanding in climate modeling. *Bulletin of the American Meteorological Society*, *86*(11), 1609–1614.

Holland, M. M., Bailey, D. A., Briegleb, B. P., Light, B., & Hunke, E. (2012). Improved sea ice shortwave radiation physics in CCSM4: The impact of melt ponds and aerosols on Arctic sea ice. *Journal of Climate*, *25*(5), 1413–1430.

Hoskins, B. J., & Karoly, D. J. (1981). The steady linear response of a spherical atmosphere to thermal and orographic forcing. *Journal of the Atmospheric Sciences*, *38*(6), 1179–1196.

Huang, R. X., Wang, W., & Liu, L. L. (2006). Decadal variability of wind-energy input to the world ocean. *Deep Sea Research Part II: Topical Studies in Oceanography*, *53*(1-2), 31–41.

Hughes, C. W., & Wilson, C. (2008). Wind work on the geostrophic ocean circulation: An observational study of the effect of small scales in the wind stress. *Journal of Geophysical Research: Oceans*, *113*(C2).

Hurrell, J. W., Holland, M. M., Gent, P. R., Ghan, S., Kay, J. E., Kushner, P. J., ... others (2013). The Community Earth System Model: a framework for collaborative research. *Bulletin of the American Meteorological Society*, *94*(9), 1339–1360.

Huybers, P., & Wunsch, C. (2003). Rectification and precession signals in the climate system. *Geophysical Research Letters*, *30*(19).

Jansen, M. F., Ferrari, R., & Mooring, T. A. (2010). Seasonal versus permanent thermocline warming by tropical cyclones. *Geophysical Research Letters*, *37*(3).

Kang, S. M., Xie, S.-P., Shin, Y., Kim, H., Hwang, Y.-T., Stuecker, M. F., ... Hawcroft, M. (2020). Walker circulation response to extratropical radiative forcing. *Science Advances*, *6*(47), eabd3021.

Large, W. G., McWilliams, J. C., & Doney, S. C. (1994). Oceanic vertical mixing: A review and a model with a nonlocal boundary layer parameterization. *Reviews of geophysics*, *32*(4), 363–403.

Larson, S. M., Buckley, M. W., & Clement, A. C. (2020). Extracting the buoyancy-driven Atlantic meridional overturning circulation. *Journal of Climate*, *33*(11), 4697–4714.

Larson, S. M., & Kirtman, B. P. (2015). Revisiting ENSO coupled instability theory and SST error growth in a fully coupled model. *Journal of Climate*, *28*(12), 4724–4742.

Larson, S. M., & Kirtman, B. P. (2017). Drivers of coupled model ENSO error dynamics and the spring predictability barrier. *Climate Dynamics*, *48*(11), 3631–3644.

Larson, S. M., & Kirtman, B. P. (2019). Linking preconditioning to extreme ENSO events and reduced ensemble spread. *Climate Dynamics*, *52*(12), 7417–7433.

Larson, S. M., Kirtman, B. P., & Vimont, D. J. (2017). A framework to decompose wind-driven biases in climate models applied to CCSM/CESM in the eastern Pacific. *Journal of Climate*, *30*(21), 8763–8782.

Larson, S. M., Okumura, Y., Bellomo, K., & Breeden, M. L. (2022). Destructive interference of ENSO on North Pacific SST and North American precipitation associated with Aleutian low variability. *Journal of Climate*, *35*(11), 3567–3585.

Larson, S. M., Pegion, K. V., & Kirtman, B. P. (2018). The South Pacific meridional mode as a thermally driven source of ENSO amplitude modulation and uncertainty. *Journal of Climate*, *31*(13), 5127–5145.

Larson, S. M., Vimont, D. J., Clement, A. C., & Kirtman, B. P. (2018). How momentum coupling affects SST variance and large-scale Pacific climate variability in CESM. *Journal of Climate*, *31*(7), 2927–2944.

Lawrence, D. M., Oleson, K. W., Flanner, M. G., Fletcher, C. G., Lawrence, P. J., Levis, S., ... Bonan, G. B. (2012). The CCSM4 land simulation, 1850–2005: Assessment of surface climate and new capabilities. *Journal of Climate*, *25*(7), 2240–2260.

Liu, F., Luo, Y., Lu, J., & Wan, X. (2017). Response of the tropical Pacific Ocean to El Niño versus global warming. *Climate Dynamics*, *48*(3), 935–956.

Liu, F., Luo, Y., Lu, J., & Wan, X. (2021). The role of ocean dynamics in the cross-equatorial energy transport under a thermal forcing in the southern ocean. *Advances in Atmospheric Sciences*, *38*, 1737–1749.

Liu, W., Lu, J., & Xie, S.-P. (2015). Understanding the Indian Ocean response to double CO_2 forcing in a coupled model. *Ocean Dynamics*, *65*(7), 1037–1046.

Liu, W., Lu, J., Xie, S.-P., & Fedorov, A. (2018). Southern Ocean heat uptake,

redistribution, and storage in a warming climate: The role of meridional overturning circulation. *Journal of Climate*, *31*(12), 4727–4743.

Lu, J., & Zhao, B. (2012). The role of oceanic feedback in the climate response to doubling CO_2. *Journal of Climate*, *25*(21), 7544–7563.

Luo, Y., Lu, J., Liu, F., & Liu, W. (2015). Understanding the El Niño-like oceanic response in the tropical Pacific to global warming. *Climate Dynamics*, *45*(7), 1945–1964.

Luongo, M. T., Xie, S.-P., & Eisenman, I. (2022a). Buoyancy forcing dominates the cross-equatorial ocean heat transport response to northern hemisphere extratropical cooling. *Journal of Climate*, *35*(20), 3071–3090.

Luongo, M. T., Xie, S.-P., & Eisenman, I. (2022b). *Data and Code from: Buoyancy Forcing Dominates the Cross-Equatorial Ocean Heat Transport Response to Northern Hemisphere Extratropical Cooling.* [CODE]. UC San Diego Digital Collections. doi: https://doi.org/10.6075/J0PR7W6B

Luongo, M. T., Xie, S.-P., Eisenman, I., Hwang, Y.-T., & Tseng, H.-Y. (2023). A Pathway for Northern Hemisphere Extratropical Cooling to Elicit a Tropical Response. *Geophysical Research Letters*, *50*(2), e2022GL100719.

Mantua, N. J., & Hare, S. R. (2002). The Pacific decadal oscillation. *Journal of Oceanography*, *58*(1), 35–44.

McMonigal, K., Larson, S., Hu, S., & Kramer, R. (2023). Historical Changes in Wind-Driven Ocean Circulation Can Accelerate Global Warming. *Geophysical Research Letters*, *50*(4), e2023GL102846.

McMonigal, K., & Larson, S. M. (2022). ENSO Explains the Link Between Indian Ocean Dipole and Meridional Ocean Heat Transport. *Geophysical Research Letters*, *49*(2), e2021GL095796.

Munk, W., & Wunsch, C. (1998). Abyssal recipes II: Energetics of tidal and wind mixing. *Deep Sea Research Part I: Oceanographic Research Papers*, *45*(12), 1977–2010.

Neale, R. B., Chen, C.-C., Gettelman, A., Lauritzen, P. H., Park, S., Williamson, D. L., ... others (2010). Description of the NCAR community atmosphere model (CAM 5.0). *NCAR Tech. Note NCAR/TN-486+ STR*, *1*(1), 1–12.

Ogata, T., Xie, S.-P., Wittenberg, A., & Sun, D.-Z. (2013). Interdecadal amplitude modulation of El Niño–Southern Oscillation and its impact on tropical Pacific

decadal variability. *Journal of Climate*, *26*(18), 7280–7297.

Okumura, Y. M. (2013). Origins of tropical Pacific decadal variability: Role of stochastic atmospheric forcing from the South Pacific. *Journal of Climate*, *26*(24), 9791–9796.

Oort, A. H., Anderson, L. A., & Peixoto, J. P. (1994). Estimates of the energy cycle of the oceans. *Journal of Geophysical Research: Oceans*, *99*(C4), 7665–7688.

Peng, Q., Xie, S.-P., Wang, D., Huang, R. X., Chen, G., Shu, Y., ... Liu, W. (2022). Surface warming–induced global acceleration of upper ocean currents. *Science Advances*, *8*(16), eabj8394.

Richter, I., Doi, T., Behera, S. K., & Keenlyside, N. (2018). On the link between mean state biases and prediction skill in the tropics: an atmospheric perspective. *Climate Dynamics*, *50*, 3355–3374.

Scott, R. B., & Xu, Y. (2009). An update on the wind power input to the surface geostrophic flow of the world ocean. *Deep Sea Research Part I: Oceanographic Research Papers*, *56*(3), 295–304.

Seo, H., O'Neill, L. W., Bourassa, M. A., Czaja, A., Drushka, K., Edson, J. B., ... others (2023). Ocean Mesoscale and Frontal-Scale Ocean–Atmosphere Interactions and Influence on Large-Scale Climate: A Review. *Journal of Climate*, *36*(7), 1981–2013.

Smith, R., Jones, P., Briegleb, B., Bryan, F., Danabasoglu, G., Dennis, J., ... others (2010). The parallel ocean program (POP) reference manual ocean component of the community climate system model (CCSM) and community earth system model (CESM). *LAUR-01853*, *141*, 1–140.

Todd, A., Zanna, L., Couldrey, M., Gregory, J., Wu, Q., Church, J. A., ... others (2020). Ocean-only FAFMIP: Understanding regional patterns of ocean heat content and dynamic sea level change. *Journal of Advances in Modeling Earth Systems*, *12*(8), e2019MS002027.

von Storch, J.-S., Sasaki, H., & Marotzke, J. (2007). Wind-generated power input to the deep ocean: An estimate using a $1/10^o$ general circulation model. *Journal of Physical Oceanography*, *37*(3), 657–672.

Wang, W., & Huang, R. X. (2004). Wind energy input to the Ekman layer. *Journal of Physical Oceanography*, *34*(5), 1267–1275.

Wunsch, C. (1998). The work done by the wind on the oceanic general circulation.

Journal of Physical Oceanography, *28*(11), 2332–2340.

Wunsch, C., & Ferrari, R. (2004). Vertical mixing, energy, and the general circulation of the oceans. *Annu. Rev. Fluid Mech.*, *36*, 281–314.

Wyrtki, K. (1975). El Niño—the dynamic response of the equatorial Pacific Ocean to atmospheric forcing. *Journal of Physical Oceanography*, *5*(4), 572–584.

Zhai, X., Johnson, H. L., Marshall, D. P., & Wunsch, C. (2012). On the wind power input to the ocean general circulation. *Journal of Physical Oceanography*, *42*(8), 1357–1365.

Zhang, Y., Yu, S., Amaya, D. J., Kosaka, Y., Larson, S. M., Wang, X., ... others (2021). Pacific meridional modes without equatorial Pacific influence. *Journal of Climate*, *34*(13), 5285–5301.